



Originally published as:

Zeeden, C., Dietze, M., Kreutzer, S. (2018): Discriminating luminescence age uncertainty composition for a robust Bayesian modelling. - *Quaternary Geochronology*, 43, pp. 30–39.

DOI: <http://doi.org/10.1016/j.quageo.2017.10.001>

Discriminating luminescence age uncertainty composition for a robust Bayesian modelling

CHRISTIAN ZEEEDEN

Chair of Physical Geography and Geoecology, Department of Geography,
RWTH Aachen University, 52056 Aachen, Germany
PSL, IMCCE, Observatoire de Paris, 75014 Paris, France

MICHAEL DIETZE

Section 5.1 Geomorphology, GFZ German Research Centre
for Geosciences, 14473 Potsdam, Germany

SEBASTIAN KREUTZER

IRAMAT-CRP2A, Université Bordeaux Montaigne, Maison de
l'Archéologie, Esplanade des Antilles, 33607 Pessac Cedex, France

November 30, 2017

Abstract

Age-depth-relationships are essential to understand expressions of Earth history. Age-depth-relationships reveal the environmental significance of (terrestrial) sediment deposits and relate them to other paleoenvironmental archives. Although luminescence-based ages are of paramount importance, their incorporation in age-depth-models is limited due to the convoluted uncertainties with unknown proportions of systematic and random parts. Here, we use an inverse modelling approach for fine-grained quartz OSL ages of loess deposits to i) generate a probability density function of the random uncertainty part and ii) use this function to recalculate and improve stratigraphically related OSL ages. Our approach can be applied to other luminescence dating techniques. Applying the algorithm to synthetic data sets generates valid results, despite an average underestimation of the relative random uncertainty by ~18 %. All tests show that precision of the inverse modelling of uncertainty parts depends only on the number of samples per dataset. By using the output of the approach on published data the precision of a late Pleistocene loess sequence chronology was improved by 21–30%.

1. INTRODUCTION

For determining the timing, duration and temporal variability of environmental change, as recorded by palaeoenvironmental archives, ages based on optically stimulated luminescence (OSL) dating are superior to other approaches (e.g., ^{14}C -dating). Moreover, luminescence dating is crucial for time scale construction for considerable parts of the Quater-

nary, since it captures the depositional process of sediment itself. For an introduction to luminescence dating see e.g., Aitken (1998) or Preusser et al. (2008). One step beyond interpreting particular depositional ages is deploying chronologies using multiple ages in any succession of deposited sediment, i.e., converting the depth or thickness domain of a deposit to the time domain, commonly referred to as age-depth-model. Numerical chronologies rep-

represent a defined transformation of stratigraphic positions/layers to time in Earth's history, giving a fundamental basis for most studies on palaeoenvironments. Age-depth-models can be constructed by linear interpolation or fitting of polynomial or spline functions to existing ages. More sophisticated Bayesian models, in the sense of allowing statistical inferences using probability models, allow for obtaining robust age-depth-models by incorporating uncertainties from sets of individual dates (e.g., Buck et al., 1991, 1992; Bronk Ramsey, 1995; Bayliss and Ramsey, 2004; Blaauw and Christen, 2011; Blaauw and Heegaard, 2012), and sometimes also assumptions on the depositional processes (Bronk Ramsey, 2009). In particular, this involves obtaining additional information inherent to the stratigraphic sequence, i.e., by applying the stratigraphic principle that deposits lower in the profile sequence are presumably older than shallower ones. The application of Bayesian methods to stratigraphies, which are in detail described in, e.g., Bronk Ramsey, (1995, 2000, 2001) and Buck et al., (1996), reduce the uncertainty of datasets with known chronological order where age probability density functions (PDF) overlap. Most commonly, this approach uses Markov Chain Monte Carlo (MCMC) simulations (cf. Gelman et al., 2014 for an introduction). Bronk Ramsey (2000, 2009) and Steier and Rom (2000) demonstrate the relevance of depositional system assumptions and specifically Bronk Ramsey (2000) points out that the results strictly represent results of applied methods. Telford et al (2004) and Blockley et al (2007) demonstrate that age-depth-models may give misleading accuracy when the spatial distance of dated layers is not small enough. It becomes generally accepted that Bayesian age models including reproducible uncertainty are more realistic than models without uncertainty estimation (Blaauw, 2010). In the past, Bayesian age modelling approaches were mainly used by the ^{14}C community (e.g., Bayliss and Ramsey, 2004; Millard, 2004), but have also been applied to archaeomagnetism (Lanos et al., 2005; Schnepf and Lanos, 2005), U/Pb dating (Mundil, 2004;

de Vleeschouwer and Parnell, 2014;), U-series dating of speleothems (Millard, 2004; Scholz and Hoffmann, 2011; Hercman and Pawlak, 2012), ESR dating (Millard, 2006a), ^{210}Pb dating (Hercman et al., 2014) and to the integration of $^{40}\text{Ar}/^{39}\text{Ar}$ ages and cyclostratigraphic durations (Meyers et al., 2012; Sageman et al., 2014). Luminescence ages have been used for Bayesian age modelling, as well (Rhodes et al., 2003; Millard, 2004, 2006b; Huntriss, 2008; Combès and Philippe, 2017), but so far this procedure received only limited attention. Millard (2004) comments on the rare use of Bayesian age models applied to other dating techniques than ^{14}C and states: "The beauty of Bayesian chronological models is their ability to combine many different types of information in a mathematically rigorous and philosophically satisfying way. It is natural therefore to extend the method to the other available dating techniques".

This limited use of Bayesian age model improvement by other dating techniques may be related to the difficulties in providing a separation of the systematic and random parts of uncertainty. Only the random uncertainty part can be used for modelling (e.g., Gradstein et al., 2004; Huntriss, 2008; Agterberg et al., 2012). Here we consider samples from individual sediment sections measured in the same laboratory and their uncertainty parts. We regard uncertainty as random, when it does not bias ages in a systematic manner towards older or younger ages. Luminescence data can be expected to gain improved precision by Bayesian methods due to its comparably high uncertainty and often overlapping probability density functions. Combinations of systematic and random uncertainty may be expected in all dating methods. Comparing datasets of different luminescence techniques (e.g., Kreutzer et al., 2012; Constantin et al., 2014; Lomax et al., 2014; Trandafir et al., 2015) are examples where both systematic and random uncertainty structures are present. For routine dating applications, the parts of uncertainty have so far not been separated in a reproducible way.

Various software packages implement

Bayesian age models, specifically for ^{14}C dating, such as OxCal (e.g., Bronk Ramsey, 1995) and ChronoModel (Vibet et al., 2016). Simulations using age distributions are employed to obtain datasets consistent with the stratigraphic principle. However, only random uncertainty should be used in such models, and model results need to be re-combined with the systematic part of uncertainty after modelling. The necessity for separating uncertainty into random and systematic parts and attempts from a physical understanding are discussed already in Aitken, (1985), but due to the unknown uncertainty structure of several parameters of the age equation (e.g., the water content which contributes significant to uncertainty) all physical models remain rough approximations.

Scope of this article is to introduce an inverse modelling approach to resolve the proportions of systematic and random uncertainty for sets of luminescence ages from individual sections. We focus on one type of terrestrial archive (Late Quaternary loess-palaeosol-sequences) and one type of luminescence dating technique (fine-grain quartz based OSL). Based on a database of published records, a PDF of the random uncertainty is created and an existing chronology is exemplarily improved. The approach is validated with synthetic data sets of known composition and applied to an empiric data set from Saxony/Germany (Kreutzer et al., 2012). The power of the here proposed method is to work even without knowing the sources of uncertainty, the means of obtaining them, and their correlation. This approach may be considered rough, but at the same time it is effective when only age results are known. This is inevitably the case if original data sets are not available.

2. METHODS

The approach consists of three parts (Fig. 1). First, a survey of published OSL chronology data sets for loess-palaeosol-sequences is integrated to a database of appropriate material. Second, based on this OSL data a PDF of the random uncertainties is generated, applying

MCMC methods, using resampling statistics. A PDF is preferred here to a fixed value of random/systematic uncertainty, as these may be different for individual ages from a dataset. Third, this PDF-based information about the random uncertainties is used in a Bayesian age-depth model to calculate more precise ages with reduced combined uncertainties. All calculations are programmed and performed using the free statistic programming language R (R Development Core Team, 2017). The two models (PDF generation and age recalculation) are written as documented functions and – together with test data sets – provided as Appendix and supplementary data repository for reproduction and modification of the results reported here. Please note that our calculations using resampling procedures; hence results vary for different experiments and may not be perfectly reproducible. Throughout this text R code snippets or function arguments are given in monospaced characters and refer to full R code provided in the supplementary material.

2.1. Data sets used for modelling

Separation of random and systematic uncertainty parts of OSL data requires a robust and sufficiently large database of dated sediment deposits. Deposits have to be stratigraphically consistent and must unambiguously allow an identification of age inversions from, e.g., morphological features of the deposits. The sediment transport process that generated the deposit should allow for well-bleached sediments prior to burial (e.g., due to atmospheric suspension transport) and should show minimal post-depositional disturbance. Accordingly, to build the empiric database we focus on OSL ages reported for well documented (mainly European) loess and loess-palaeosol sequences that show high accumulation rates, especially during the last glacial maximum (Rousseau et al., 2007; Buggle et al., 2009; Újvári et al., 2010). Furthermore, aeolian sediments can be expected as sufficiently bleached before deposition. The selection of the datasets was based on a series of rig-

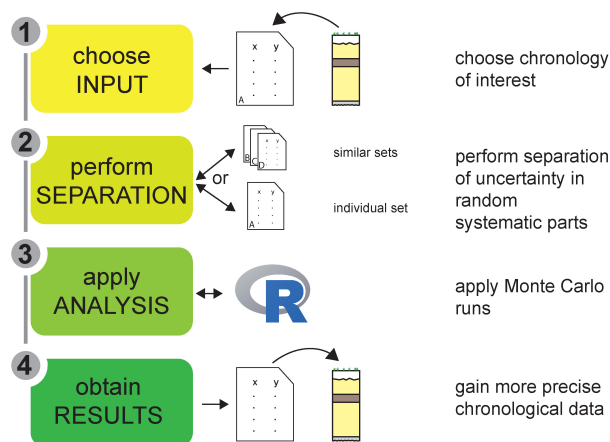


Figure 1: Flow chart of the calculation procedure.

orous constraints: (1) Only OSL age estimates obtained by fine grain (4–11 μm) quartz dating using the single aliquot regenerative-dose (SAR) approach (Murray and Wintle, 2000) are considered, (2) ages showing an equivalent dose (D_e) higher than 150 Gy are neglected (equivalent to a maximum age of about 50 ka in a loess section, depending on the environmental radioactivity), (3) only records with limited pedogenic disturbances are used. The first constraints are introduced to avoid dealing with systematic methodological uncertainties that may not be comparable, and may not be fully understood from a physical perspective. Setting a cut-off level for D_e at 150 Gy is somewhat arbitrary and a balance between data availability and suggested higher reliability of lower D_e values. The mineral quartz was chosen because it is supposed not to suffer from an anomalous signal loss over time (athermal fading, an effect that leads to age underestimation; Wintle, 1973). Further, the limitation to D_e values < 150 Gy accounts for the reported and expected dose saturation levels of quartz in general, which range from about 125 Gy up to about 400 Gy in exceptional cases (cf. Buylaert et al., 2007; Roberts, 2008; Chapot et al., 2012). This limit is kept for all datasets; even when a study reported locally higher saturation levels.

2.2. Probability density function for random uncertainty part

When investigating sediment samples with a similar source area and deposition history, age inversions within a concordant sediment section may be explained at first order by the random uncertainty of a dating method. Any dating method with inherent random uncertainty is expected to show age inversions. Thereby, the number of inversions should only depend on the proportion of random uncertainty for the dated samples, whereas systematic uncertainty causes bias in one direction (old/young) and does not contribute to age inversions. To create a synthetic record with imposed uncertainty, ages of datasets are ordered. Accordingly, for each data set random uncertainties, ranging from 1 % to 100 % (and systematic uncertainties vice versa) are tested for their ability to explain the observed number of age inversions. The tests included for each combination of uncertainty parts, realised as a sequence of integer percentages of random uncertainty ($n = 100$), 1001 times ($n.MC = 1001$) resampling the natural dataset with the given uncertainty properties. All random uncertainty parts that could explain the empiric number of age inversions were given a relative probability, representing a measure for the number of simulations in agreement with real luminescence

data and their number of inversions (Fig. 2). Fig. 2A depicts the PDF for all here considered datasets, and Fig. 2B represents the PDF from a single dataset by Kreuzer et al. (2012). The function `create.pdf` uses datasets and their 1-sigma uncertainty as input, because most datasets are published with this uncertainty level. In summary, we test different amounts of random uncertainty (in %) for their possibility to create the number of observed age inversions. This is done using simulations of reported ages and their uncertainty. Noisy PDFs can be result of sparse simulation cases consistent with data, and also unclear density due to a limited number of simulations. In some cases, this can be countered by increasing the number of simulations where computer memory allows.

2.3. Algorithm validation

Synthetic data sets are created to explore the validity and performance of the uncertainty separation algorithm. Questions to be addressed concern the influence of the number of samples in a dataset, the number of different data sets, the proximity of individual ages to each other and the overall size of the relative uncertainty on the shape of the random uncertainty density function. The supplementary materials contain a series of R-scripts that are devoted resolving these questions and may be used by the reader to comprehend and extend the tests (Fig. 3).

To estimate the overall scatter introduced by the technique, a Monte Carlo design with 500 repeated simulations of one data set with 35 samples was created. The samples in this data set are all separated by 500 years, starting from zero, have a relative uncertainty of 12 % and a random uncertainty part of 50 %. Based on these parameters, in each Monte Carlo run normal distributed random numbers were generated with the means defined by the evenly spaced ages and the standard deviations defined by the random uncertainty parts of the relative uncertainty.

To test the influence of age offsets within a chronology (i.e., effect of sampling den-

sity or deposition rate; see Fig. B, Supplementary script `04_test_age_offset.R`), the spacing of individual ages was changed from 5 years to 50,000 years. The limits of this range are far from being realistically encountered in any empiric data set but highlight the behaviour of the algorithm also in extreme cases. To test the influence of the sample size, their number in a data set was changed from 5 to 50 (logarithmically increasing; see Fig. 3C and Supplementary script `05_test_number_of_samples.R`). The upper limit of this range will be encountered only in few empiric data sets and is primarily used to show the influence of this parameter. The influence of number of empiric data sets (i.e., size of the data base; see Fig. 3D and Supplementary script `06_test_number_of_data_sets.R`) was tested by changing the data base size from 5 to 200. In a last test, the relative uncertainty was changed from 0 % to 100 % in integer steps to test the influence of this parameter; see Fig. 3E and Supplementary script `07_test_random_uncert_part.R`.

2.4. Recalculating luminescence ages

Buck et al. (1991) introduced the consideration of the principle of stratigraphy in a statistical way to ^{14}C dating, and the concept has been described in detail various times thereafter (e.g., Buck et al., 1991, 1992; Bronk Ramsey, 1995; 2000; Steier and Rom, 2000; Blockley et al., 2004). Here, the PDF as derived from the empirical data set is used to generate random uncertainty parts and assign them to a series of empiric ages in stratigraphic order. The respective systematic uncertainty part is stored separately and is not used for the following age-depth modelling procedure, but is re-combined with the final result. This procedure is applied to in total as many simulation runs as necessary to gain `n.MC.min` (default:1000) stratigraphically consistent data sets. The routine `recalculate.ages` estimates the number of required MCMC runs based on a subsample size and improves computational efficiency through vectorisation of the calculations

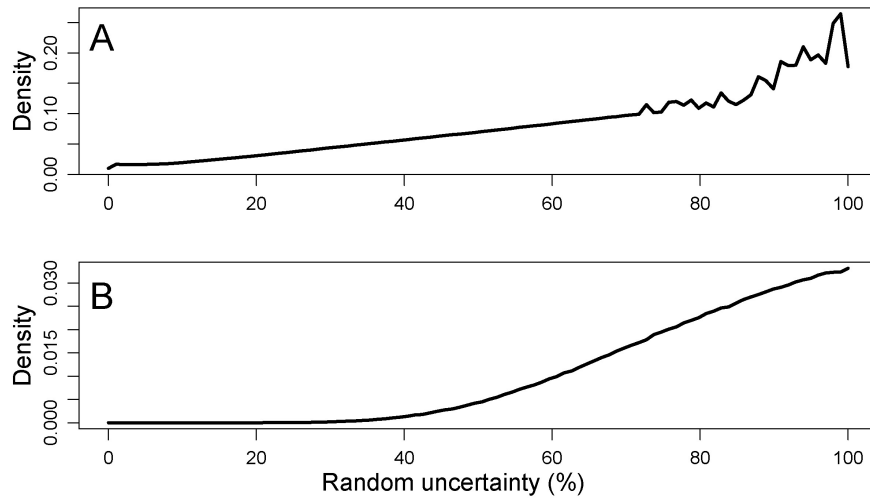


Figure 2: Probability density functions (PDFs) of random uncertainties using all input data (A), and only one specific dataset (Kreutzer et al. 2012; B). The relative density (ordinate) is plotted versus the percentage of random uncertainty (abscissa). Note that the PDF of all used data (A) allows for the whole range from 0 to 100 %, while the PDF from the dataset by Kreutzer et al. (2012; B) shows an increasing density with random uncertainty from ca. 30 % onwards.

in R. Depending on the likelihood to draw inverted ages from the input data description, this can involve a large number of Monte Carlo runs, which are cut by a parameter `n.MC.max` to avoid longer than necessary processing. The `recalculate.ages` routine uses the 2-sigma uncertainty of data as input, and by default provides 95 % uncertainty of the Bayesian model result; the output probabilities can be set by adjusting the probability parameter. It calculates a maximum of `n.MC.max` times `n.MC.min` simulations.

Straightforward interpretation of resulting simulations with stratigraphically consistent data are problematic (cf. Bronk Ramsey, 2000, 2009; Steier and Rom, 2000). Uncorrected results from MCMC simulations have a higher probability for results with relatively long durations exceeding means of original maximum and minimum ages (and producing datasets with youngest ages shifted towards younger ages, and the oldest age being shifted towards the older end). To account for this effect, the Bayesian weighting prior for ordered data sets is defined according to (Bronk Ramsey, 2000,

2009): $P = (t_{max} - t_{min}) - n$, where t_{max} is the oldest sample age, t_{min} the youngest sample age and n is the number of ages/samples, including the introduction of two boundary ages to counter effects of preferring long durations (e.g., Bronk Ramsey, 2000). For unordered datasets P was set to 0, as outlined, e.g., in Bronk Ramsey (2000). Furthermore, two outer boundary ages are set at a distance of five times the mean temporal spacing of samples (similar to boundaries in OxCal; Bronk Ramsey, 2009). Fig. 4 shows how the applied algorithm avoids preferring long durations and successfully accounts for this issue.

However, this effect may affect results from other datasets with other data structures. Specifically, the pattern of inversions and age non-equidistant distance between samples (or clustering of samples at specific age intervals) may influence this effect. Summarizing, the re-calculation of OSL ages represents an age-depth model using the mentioned Bayesian Prior and a PDF of the random and systematic parts of uncertainty.

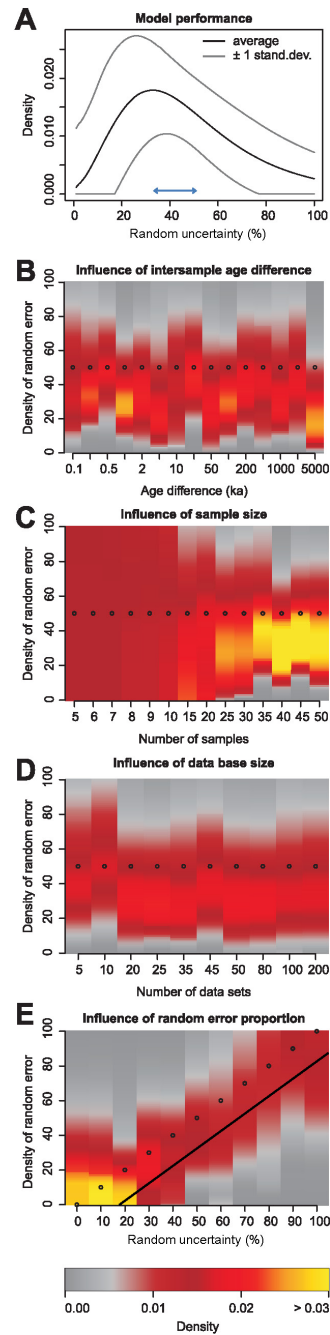


Figure 3: Algorithm validation results for synthetic datasets with 50 % random uncertainty. A: Mean (black line) and standard deviation (grey lines) values for PDF generated by 500 model runs with identical input parameters, the arrow indicates the difference between model input and output, B: Influence of age difference between samples, C: Influence of sample size, D: Influence of data base size and E: Influence of the random uncertainty proportion, the line indicates results lowered by about 18 %. Black dots overlaying image plots indicate the input value of random uncertainty part (0.5/50 %) in B-E.

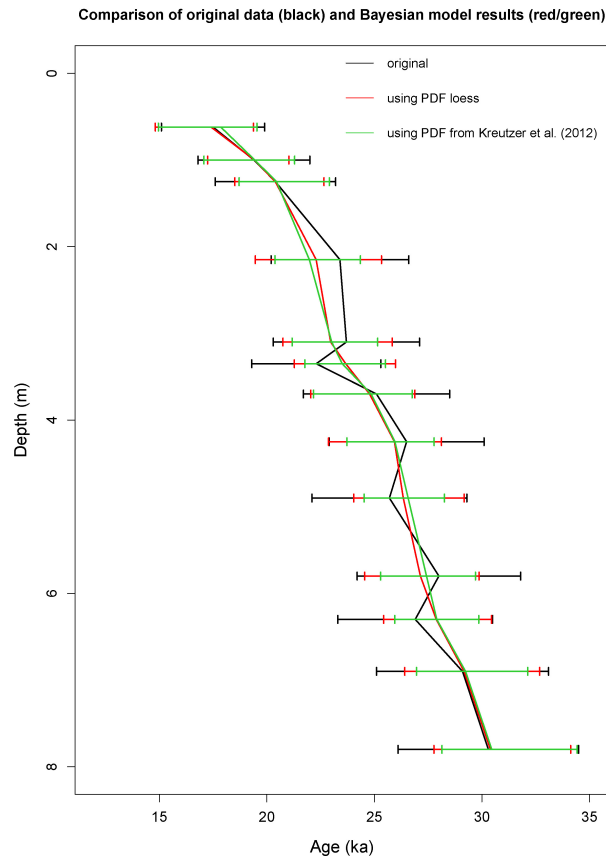


Figure 4: Comparison of the original chronology by Kreutzer et al., 2012 (black) and the results from our approach including usage of a PDF for estimating systematic and random parts of uncertainty and following Bayesian analysis (red, for PDF from all data; green for the PDF from this dataset). Usage of the PDF from the dataset by Kreutzer et al., 2012 results in systematically higher precision than the PDF of all data.

3. RESULTS

3.1. Algorithm validation

Results from 500 repeated model-runs with identical input parameters show a high probability density between 25 % and 40 % random uncertainty (maximum around a random uncertainty of 35 %). These results imply an underestimation of the true random uncertainty part by 10 % to 25 % (18 % on average, cf. Figs. 3a (see the peak at 38 % instead of 50 %, indicated by the arrow), 3e (see colours representing high density systematically below the 50 % dots, the line indicates the 18 % lowered

density), and supplementary materials). The density curve is asymmetric with a negative skew. Age differences between samples do not influence the model results (Fig. 3B). The rather stable underestimate of about 18 % is observed regardless of the age difference between samples, and thus the potentially existing age inversions due to random uncertainty (see specifically Fig. 3A & 3E). Sample size has a significant impact on model results (Fig. 3c). With less than about 10 samples per dataset the PDF is rather flat. It indicates basically any proportions of random and systematic uncertainty are equally likely. From about 15 samples onward, the PDF becomes systemat-

ically narrower. However, even as many as 50 samples do not influence the observed underestimation. The size of a data base (i.e., the number of individual datasets) does not influence the model results. Despite the about 18 % underestimation effect our approach reliably detects all imposed random uncertainty proportions (Fig. 3e).

3.2. Inverse modelling

Data regarded reliable by the authors and fulfilling the criteria outlined in section 2.1 are contained in publications by ChongYi et al., 2012; Constantin et al., 2014, 2015; Fuchs et al., 2013; Kreutzer et al., 2012; Lu et al., 2007 (one age fulfills criteria but is not regarded as robust by the authors); Meszner et al., 2013; Timar-Gabor et al., 2011. For unknown reasons the dataset by Meszner et al., (2013) suggests random uncertainty to largely exceed the overall uncertainty (see supplementary Fig. 1). Thus, we excluded this dataset from further analysis. These sets were used to create a PDF for fine grain OSL ages of the sediment type loess. The empiric PDF (PDF_{Loess} , Table 1, Fig. 2a) reveals that high percentages of random uncertainty have a higher probability than low percentages of random uncertainty. The PDF generated from all input data sets, hereafter termed " PDF_{Loess} ", shows an almost linearly increasing probability for higher contributions of random uncertainty. Applying the approach to a single data set (Kreutzer et al., 2012) yields different results (Fig. 2b). There, the PDF has the highest probability for high random uncertainty percentages and declines with lower values. The PDF approaches zero for values smaller than about 30 % random uncertainty.

3.3. Application to an empiric data set

Results of the original and refined chronologies of the empiric data set from Ostrau/Saxony (Kreutzer et al., 2012, Fig. 4) reveal that the overall uncertainty of the data could be reduced on average by 30 % when using the PDF

from this specific dataset, and by 21 % when using the PDF from all input data sets (PDF_{Loess} ; Table 1). The improvement is expressed as the difference between the uncertainty after modelling and the original uncertainty over the original uncertainty (all 2-sigma). Data near the top and bottom of the sediment section cannot be improved to a similar extent as data in between (Table 2 and Fig. 4).

4. DISCUSSION

4.1. Methodological considerations

Investigating synthetic datasets (cf. Sections 2.4 and 3.1) shows a wide, slightly negatively skewed distribution of random uncertainty for datasets of realistic sample numbers (Fig. 3). For small numbers of samples, the distribution becomes flat over the entire uncertainty proportion range. The number of age inversions in a data set is an integer number; any specific number of age inversions generates a specific result with uncertainty. Generally, it may be presumed that higher numbers of age inversions represent higher random uncertainty. Thus, the more ages an individual dataset comprises, the higher becomes the precision of the inverse modelling approach (Fig. 3C). The synthetic data consistently show that our approach underestimates random uncertainty by about 18 %. We attribute this underestimation to the assumption that real luminescence ages may be approximated by sorted surrogates of a given datasets. This implementation inevitably leads to a smaller number of inversions and therefore less random uncertainty than originating from resampling real ages. However, in the absence of precise knowledge about real ages this approach is the only and best available option in our opinion. Robustness of the approach towards age differences between samples and overall data set size is encouraging with respect to a wider application to other sediment types and luminescence dating techniques. It accounts for all potential causes of unresolvable dating issues. It is the number of samples per data set that matters. Thus, highly

Table 1: Data of the PDF_{Loess}, a probability density function established from fine grain OSL quartz data from loess-palaeosol sequences. The first column gives the percentage of the random uncertainty; the second column shows the respective probability. Please note that this PDF was created using a simulation approach, and therefore attempts to reconstruct this dataset using the supplementary R functions is expected to lead to similar, but not the same results. For a visualisation see Fig. 2A.

uncertainty [%]	probability	uncertainty [%]	probability	uncertainty [%]	probability
0	0.01000628	33.333333	0.04821316	66.666667	0.09243584
1.010101	0.016541	34.343434	0.04934387	67.676768	0.09411864
2.020202	0.01645952	35.353535	0.05076916	68.686869	0.09503695
3.030303	0.01645641	36.363636	0.05197299	69.69697	0.09674894
4.040404	0.01644975	37.373737	0.05350727	70.707071	0.09791893
5.050505	0.01644684	38.383838	0.0543716	71.717172	0.09893429
6.060606	0.0167408	39.393939	0.05586333	72.727273	0.11468022
7.070707	0.01720838	40.40404	0.05712714	73.737374	0.10165718
8.080808	0.01769127	41.414141	0.05872534	74.747475	0.1027008
9.090909	0.01850702	42.424242	0.05997554	75.757576	0.11876968
10.10101	0.01949214	43.434343	0.06107018	76.767677	0.11997022
11.111111	0.02069329	44.444444	0.06266646	77.777778	0.11389758
12.121212	0.02177999	45.454545	0.06405702	78.787879	0.12238049
13.131313	0.02283053	46.464646	0.06540718	79.79798	0.10880839
14.141414	0.02402877	47.474747	0.06628864	80.808081	0.1175924
15.151515	0.02512093	48.484848	0.06753321	81.818182	0.11098616
16.161616	0.02631646	49.494949	0.06883373	82.828283	0.13406463
17.171717	0.02733976	50.505051	0.07050314	83.838384	0.12053686
18.181818	0.02867175	51.515152	0.07177392	84.848485	0.1149341
19.191919	0.02969268	52.525253	0.07315606	85.858586	0.12210364
20.20202	0.03105637	53.535354	0.07441017	86.868687	0.13114198
21.212121	0.03223179	54.545455	0.07580185	87.878788	0.16076203
22.222222	0.03365747	55.555556	0.07761307	88.888889	0.15430351
23.232323	0.03498134	56.565657	0.07876972	89.89899	0.14087445
24.242424	0.03605716	57.575758	0.08015879	90.909091	0.18570389
25.252525	0.0375575	58.585859	0.08125125	91.919192	0.17900544
26.262626	0.03893187	59.59596	0.08261136	92.929293	0.17969401
27.272727	0.03998447	60.606061	0.08435207	93.939394	0.20995126
28.282828	0.04152177	61.616162	0.08569958	94.949495	0.18861811
29.292929	0.04302369	62.626263	0.08709216	95.959596	0.19655025
30.30303	0.044297	63.636364	0.08836269	96.969697	0.18295683
31.313131	0.04546706	64.646465	0.08982048	97.979798	0.24858113
32.323232	0.04657738	65.656566	0.09097122	98.989899	0.26420855

Table 2: Data and associated uncertainty from Kreutzer et al. (2012), and improved precision as by the methods outlined.

sample	Original data		PDF of all loess datasets			PDF Kreutzer et al. (2012) data				
	Depth	Age	1 σ	2 σ	mean age	lower σ	upper σ	mean age	lower σ	upper σ
boundary										
BT607	0.15	15.1	1.4	2.8	15.01	12.10	17.71	15.23	11.44	18.00
BT608	0.62	17.5	1.2	2.4	17.41	14.81	19.38	17.86	14.96	19.54
BT609	1	19.4	1.3	2.6	19.43	17.25	21.03	19.44	17.08	21.29
BT610	1.25	20.4	1.4	2.8	20.40	18.51	22.66	20.45	18.71	22.91
BT611	2.15	23.4	1.6	3.2	22.29	19.47	25.33	21.98	20.38	24.35
BT612	3.1	23.7	1.7	3.4	22.97	20.75	25.83	23.02	21.18	25.15
BT613	3.35	22.3	1.5	3	23.67	21.28	25.98	23.51	21.77	25.52
BT614	3.7	25.1	1.7	3.4	24.78	22.04	26.88	24.85	22.17	26.76
BT615	4.25	26.5	1.8	3.6	25.93	22.87	28.12	25.96	23.73	27.78
BT616	4.9	25.7	1.8	3.6	26.35	24.04	29.18	26.57	24.53	28.26
BT626	5.8	28	1.9	3.8	27.14	24.55	29.87	27.42	25.29	29.70
BT625	6.3	26.9	1.8	3.6	27.88	25.43	30.45	27.90	25.95	29.85
BT624	6.9	29.1	2	4	29.17	26.41	32.68	29.24	26.96	32.13
BT622	7.8	30.3	2.1	4.2	30.39	27.77	34.13	30.46	28.14	34.43
boundary										

resolved (and sampled) sediment sections are ideal for expanding the approach to further deposit types and measurement techniques.

The size of the database does not play a role for PDFs from multiple datasets when these PDFs are of similar structure (number of ages, age difference; Fig. 3D). However, because hardly ever only datasets of the same length are in a data compilation, we regard building a database representative for a dating technique useful.

4.2. Properties of probability density functions

The PDF_{Loess} (Fig. 2A) shows higher probabilities of higher random uncertainties. Even fully systematic uncertainty is possible, though unlikely (see table 1 and PDFs in Fig. 2). It may be subject to personal considerations whether (A) it is more appropriate to use a PDF from multiple datasets with similar sedimentologic origin and dating approach (here: fine grain OSL Quartz data from loess-palaeosol sequences) or (B) a PDF of an individual dataset (if suf-

ficient dates are available, as for example in the dataset by Kreutzer et al. (2012), Fig. 2B) to estimate a PDF of random uncertainty. We advocate for using both, a PDF from an individual dataset and a PDF compiled from a set of representative datasets. The probability density functions of both concepts overlap in our case, and the impact on the age recalculations are similar, though smaller uncertainties result from the PDF from the dataset by Kreutzer et al. (2012).

The constructed PDF for loess (PDF_{Loess}, Fig.2A) is assumed to be representative only for fine grain OSL quartz ages from loess and loess-palaeosol sequences, and may exclusively be used for such environmental archives. More or different data used for future inverse modelling approaches may modify results, and therefore also results of age-depth models based on this PDF. Here we set the maximum percentage of random uncertainty to 100 %. However, if the OSL uncertainty is systematically underestimated, also higher percentages should be used. Such a possibility is explored by setting the maximal random uncertainty to

1000 %, along with an artificial dataset where random uncertainty is explored up to 500 % (Fig. 5). A maximum in the random part of uncertainty is located at 120 % for both PDFs. Because the method tends to underestimate random uncertainty, and also systematic uncertainty can be expected (e.g., Constantin et al. 2015), these results point at an even larger underestimation of uncertainty in the analysed luminescence datasets. A closer investigation in this direction is, however, clearly not aim of this manuscript, but may lie in the integration of the time dependent water content since deposition.

A direct comparison to the information on the systematic and random uncertainty, as given by Constantin et al. (2014), is difficult in detail because of their deterministically set percentage versus the PDFs derived by our approach. A dominance of systematic uncertainty as proposed by Constantin et al. (2014) is possible, given that the PDF from the dataset by Constantin et al. (2014, see Fig. 6) allows for all possible uncertainty percentages. However, the proposed approach results in highest probabilities for random uncertainty of 120 %.

4.3. Improved precision of the empiric data set

The increase in precision due to the Bayesian Prior of superposition is related to the amount of random uncertainty. The higher the random uncertainty, the higher is the improvement by the statistical method. The age recalculation removed all age inversions inherent to the initial dataset when considering the mean ages. However, more important are the changes of the age-depth relationship between 1 m and 3 m depth and the increase in the accumulation rate between 3 m and 4 m depth (Fig. 4). The recalculated dataset now reveals up to four different phases of sedimentation: (1) 0–1.5 m, (2) 1.5–3 m, (3) 3–4 m and (4) 4–8 m. Phases of rapid sedimentation (2 and 4) are linked to the corresponding loess layers. The recalculated results are not changing the palaeoenvironmental interpretation by Kreuzer et al. (2012), how-

ever, they more sharply reveal the significance of the sedimentation phases. In combination with other datasets, this outcome has potential to further constraining the European climate history. Nevertheless, our results also show the limitation of our approach: The improvement of a single dataset does not necessarily lead to a changed palaeoenvironmental history.

4.4. General application of Bayesian age depth models

The application of a simulation allows only stratigraphically consistent data in a statistically justified way. Separating random and systematic uncertainty for luminescence data, can advance the precision of chronologies without decisively increasing precision in unjustified ways as specifically assuming uncertainty to be fully random. The accuracy depends on the systematic part of data uncertainty. We presume that all datasets with overlapping probability density functions of ages can be improved this way. The degree of data improvement depends on the shape of the PDF, the amount of overlap of age uncertainties and the number of measured ages of the chronology. The differentiation of clustered ages and/or hiatuses obvious from lithology is useful, and can be incorporated in algorithms, as available in the OxCal software (e.g., Bronk Ramsey, (1995) or ChronoModel (<http://www.chronomodel.fr>; manual: Vibet et al., 2016). A more comprehensive database for a PDF_{Loess} would be advantageous. However, more important would be the generation of decisively large datasets for single sediment sections. Unfortunately, only a few sections appear to be dated with the sufficient high resolution (e.g., at least every 50 cm; if stratigraphically applicable). We aim at finding a balance between the number and size of datasets and the needed constraints to generate reliable output. Regardless of whatever input PDF is used, resampling specific datasets will tend to show stratigraphically consistent results for a specific range of random and systematic uncertainty which may better explain a given dataset.

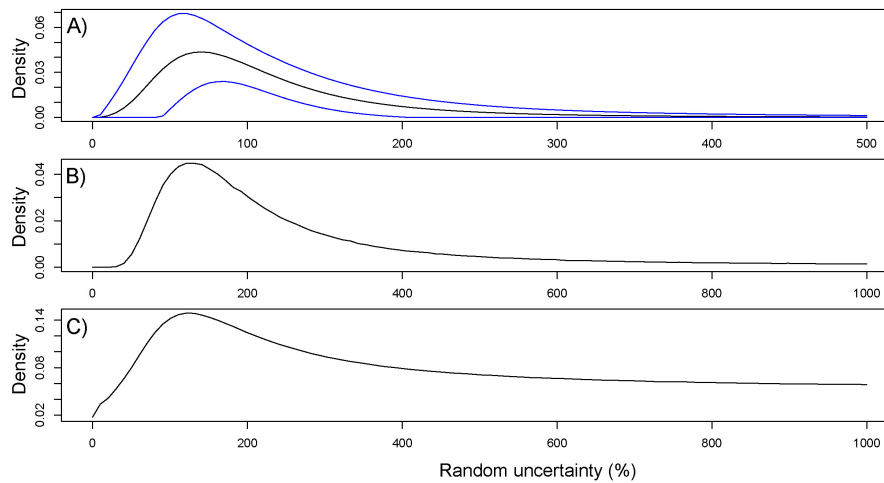


Figure 5: Exploring random uncertainty beyond 100 % of reported uncertainty (at 95 % confidence level). (A) represents an artificial sample with 100 % random uncertainty. (B) and (C) explore random uncertainty up to 10 times the reported uncertainty for the PDFs from one dataset (B; Kreutzer et al. 2012) and all here investigated datasets (C). Note that the abscissas in A) and B, C) have different labels.

In contrast to calibrated ^{14}C ages with complex PDF shapes, the OSL data used here are assumed to be normal distributed around a mean. This normal distribution has the advantage that improbable data structures do not need to be considered outliers. Other and more complex distributions and also density functions may be used in adjusted computer code, but are not commonly reported for luminescence ages. However, this also limits the increase in precision by applying Bayesian methods to luminescence dates.

4.5. Parametrizing uncertainty for Bayesian age depth models

Dating techniques relying on standards and constants have an overall uncertainty with parts of uncertainty being systematic and parts being random. Tests with synthetic data showed that datasets comprising a low number of ages lead to PDFs allowing for systematic and random uncertainty in the whole range between 0 % and 100 %. In cases where the amount of random/systematic uncertainty is unknown, we suggest to conservatively draw random/systematic uncertainty from a uni-

form PDF from 0 % to 100 % or use dataset-specific PDFs once these are generated or compiled from the literature. Higher systematic uncertainties lead to relatively imprecise results of Bayesian age depth-models and vice versa.

4.6. Critical considerations and limitations

With our approach, the random and systematic parts of uncertainty are not strictly separated for every single age, but a PDF is modelled for all ages; either of one data set or a suite of data sets with comparable genetic constraints. This approach may systematically fail to hit the correct random and systematic uncertainty parts for individual dates, but is a generalisation made to adequately describe a data set. Likewise, a dataset with a small number of ages will not generate a narrow PDF. However, since the amount of random and systematic parts of uncertainty can be different for individual dates of a chronology, we do not consider imprecise PDFs as problematic, but rather a realistic case. Moreover, especially PDFs resulting from short chronologies should be regarded

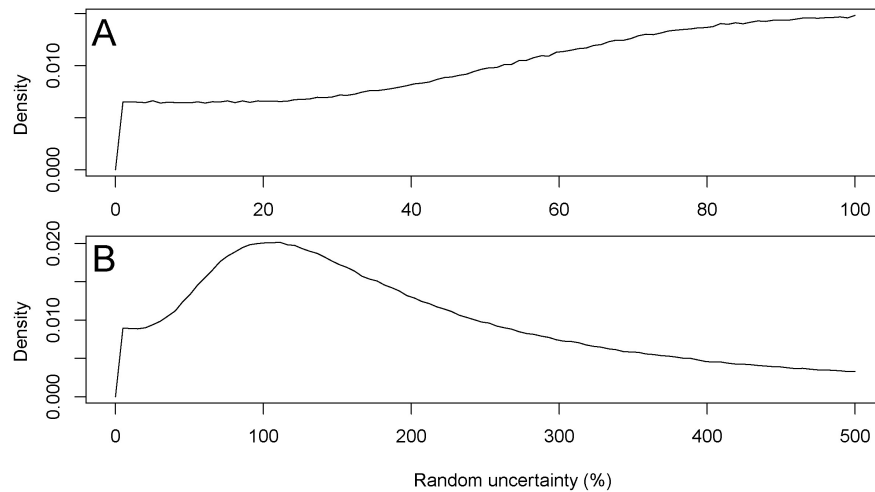


Figure 6: PDFs for the dataset by Constantin et al. (2014). (A) represents a PDF of the random uncertainty proportion from 1–100 %, (B) explores a wider random uncertainty proportion up to 500 %.

carefully when the uncertainty is expected to be dominantly systematic. Finally, Bayesian age models are expected to produce results with an improved precision, in comparison to the original data. Nevertheless, this precision may become misleading if potential systematic uncertainties have been not included by the individual dates (or dating methods; e.g. systematically higher or lower water content than assumed for luminescence). Further, computation results should be interpreted as a result of the applied method, and not necessarily as a perfect estimate of the true precisions; see Bronk Ramsey, (2000) for a thorough discussion of what Bayesian ages stand for. Though the choice of a uniform Bayesian prior distribution is applied here, it is neither the only option (Bronk Ramsey, 2000; 2009), nor may it be in all cases the preferred one (e.g., Bronk Ramsey, 2000). However, it may be assumed as the most appropriate option if no additional information on this distribution is available. Independent determination of the minimum and maximum systematic (or random) uncertainty for luminescence data derived from physical processes (as e.g., decay constants) would be beneficial for future work, and has the potential to improve on the here presented PDFs

by setting the limits parameter in the function `recalculate.ages`.

5. CONCLUSIONS

Using a combination of an inverse modelling approach to estimate the random and systematic parts of OSL data uncertainty and a Bayesian age-depth model, we increase the precision of fine grain quartz OSL chronologies. Where separation of uncertainty into random and systematic parts is impossible, we propose to use a uniform PDF allowing for random uncertainty between 0 % and 100 %. Exemplary the precision of ages has been improved by 21–30 %, depending on the PDF used for random/systematic uncertainty. The applied approach of separating uncertainty parts of luminescence data may be applied to other environmental archives such as fluvial, limnic and marine datasets, and to other (luminescence) dating techniques. The application of the presented approach leads to a higher precision of luminescence-based chrono-stratigraphies, allowing more detailed conclusions about the timing and duration of Earth surface dynamics as preserved by sedimentological records.

Implementation of the approach using free

and open software allows for a maximum of transparency and reproducibility. Adaptation of the provided functions for and application to new data sets (other OSL measurement protocols and techniques, other dosimeters, etc.) is encouraged and shall result in an active discussion of uncertainty patterns across these data sets.

6. ACKNOWLEDGEMENTS

This investigation was carried out in the context of the CRC 806 "Our way to Europe", supported by the DFG [Deutsche Forschungsgemeinschaft, grant number INST 216/596-2]. The work of SK is financed by a programme supported by the ANR - n° ANR-10-LABX-52. CZ is supported by a PSL fellowship. We thank Frank Preusser and two anonymous reviewers for constructive editorial work and for their valuable comments improving this manuscript.

7. REFERENCES

- Agterberg, F.P., Hammer, O., Gradstein, F.M., 2012. Chapter 14 - Statistical Procedures, in: Gradstein, F.M., Ogg, J.G., Schmitz, M.D., Ogg, G.M. (Eds.), *The Geologic Time Scale*. Elsevier, Boston, pp. 269–273.
- Aitken, M.J., 1998. *Introduction to optical dating: the dating of Quaternary sediments by the use of photon-stimulated luminescence*. Clarendon Press.
- Aitken, M.J., 1985. *Thermoluminescence dating*. Academic Press.
- Bayliss, A., Ramsey, C.B., 2004. Pragmatic Bayesians: a Decade of Integrating Radiocarbon Dates into Chronological Models, in: Buck, C.E., Millard, A.R. (Eds.), *Tools for Constructing Chronologies, Lecture Notes in Statistics*. Springer London, pp. 25–41.
- Blaauw, M., 2010. Methods and code for "classical" age-modelling of radiocarbon sequences. *Quaternary Geochronology* 5, 512–518. doi:10.1016/j.quageo.2010.01.002
- Blaauw, M., Christen, J.A., 2011. Flexible paleoclimate age-depth models using an autoregressive gamma process. *Bayesian Anal.* 6, 457–474. doi:10.1214/ba/1339616472
- Blaauw, M., Heegaard, E., 2012. Estimation of Age-Depth Relationships, in: Birks, H.J.B., Lotter, A.F., Juggins, S., Smol, J.P. (Eds.), *Tracking Environmental Change Using Lake Sediments, Developments in Paleoenvironmental Research*. Springer Netherlands, pp. 379–413.
- Blockley, S.P.E., Blaauw, M., Bronk Ramsey, C., van der Plicht, J., 2007. Building and testing age models for radiocarbon dates in Lateglacial and Early Holocene sediments. *Quaternary Science Reviews* 26, 1915–1926. doi:10.1016/j.quascirev.2007.06.007
- Blockley, S.P.E., Lowe, J.J., Walker, M.J.C., Asioli, A., Trincardi, F., Coope, G.R., Donahue, R.E., 2004. Bayesian analysis of radiocarbon chronologies: examples from the European Late-glacial. *J. Quaternary Sci.* 19, 159–175. doi:10.1002/jqs.820
- Bronk Ramsey, C., 2009. Bayesian Analysis of Radiocarbon Dates. *Radiocarbon* 51, 337–360.
- Bronk Ramsey, C., 2001. Development of the radiocarbon calibration program. *Radiocarbon* 43, 355–363.
- Bronk Ramsey, C., 2000. Comment on "The use of Bayesian Statistics for ^{14}C Dates of Chronologically ordered samples: A Critical Analysis." *Radiocarbon* 42, 199–202.
- Bronk Ramsey, C., 1995. Radiocarbon calibration and analysis of stratigraphy. The OxCal program. *Radiocarbon* 37, 425–430.
- Buck, C.E., Cavanagh, G., Litton, C., 1996. *Bayesian Approach to Interpreting Archaeological Data*. Wiley.
- Buck, C.E., Kenworthy, J.B., Litton, C.D., Smith, A.F.M., 1991. Combining Archaeological and Radiocarbon Information. A Bayesian Approach to Calibration. *Antiquity* 65, 808–821.
- Buck, C.E., Litton, C.D., Smith, A.F.M., 1992. Calibration of radiocarbon results pertaining to related archaeological events. *Journal of Archaeological Science* 19, 497–512. doi:10.1016/0305-4403(92)90025-X
- Buggle, B., Hambach, U., Glaser, B., Gerasimenko, N., Marković, S., Glaser, I., Zöller, L., 2009. Stratigraphy, and spatial

and temporal paleoclimatic trends in South-eastern/Eastern European loess–paleosol sequences. *Quaternary International* 196, 86–106. doi:10.1016/j.quaint.2008.07.013

Buylaert, J.-P., Vandenberghe, D., Murray, A.S., Huot, S., De Corte, F., Van den Haute, P., 2007. Luminescence dating of old (> 70ka) Chinese loess: A comparison of single-aliquot OSL and IRSL techniques. *Quaternary Geochronology* 2, 9–14.

Chapot, M.S., Roberts, H.M., Duller, G.A.T., Lai, Z.P., 2012. A comparison of natural- and laboratory-generated dose response curves for quartz optically stimulated luminescence signals from Chinese Loess. *Radiation Measurements* 47, 1045–1052. doi:10.1016/j.radmeas.2012.09.001

ChongYi, E., Lai, Z., Sun, Y., Hou, G., Yu, L., Wu, C., 2012. A luminescence dating study of loess deposits from the Yili River basin in western China. *Quaternary Geochronology* 10, 50–55. doi:10.1016/j.quageo.2012.04.022

Combès, B., Philippe, A., 2017. Bayesian analysis of individual and systematic multiplicative errors for estimating ages with stratigraphic constraints in optically stimulated luminescence dating. *Quaternary Geochronology* 39, 24–34.

Constantin, D., Begy, R., Vasiliniuc, S., Panaiotu, C., Necula, C., Codrea, V., Timar-Gabor, A., 2014. High-resolution OSL dating of the Costine-Åşti section (Dobrogea, SE Romania) using fine and coarse quartz. *Quaternary International* 334–335, 20–29. doi:10.1016/j.quaint.2013.06.016

Constantin, D., Camenita, A., Panaiotu, C., Necula, C., Codrea, V., Timar-Gabor, A., 2015. Fine and coarse-quartz SAR-OSL dating of Last Glacial loess in Southern Romania. *Quaternary International* 357, 33–43. doi:10.1016/j.quaint.2014.07.052

de Vleeschouwer, D., Parnell, A.C., 2014. Reducing time-scale uncertainty for the Devonian by integrating astrochronology and Bayesian statistics. *Geology* 42, 491–494. doi:10.1130/G35618.1

Fuchs, M., Kreutzer, S., Rousseau, D.-D., Antoine, P., Hattè, C., Lagroix, F., Moine, O., Gau-

thier, C., Svoboda, J., Lisá, L., 2013. The loess sequence of Dolní Věstonice, Czech Republic: A new OSL-based chronology of the Last Climatic Cycle: Loess sequence of Dolní Věstonice, Czech Republic: OSL chronology. *Boreas* 42, 664–677. doi:10.1111/j.1502-3885.2012.00299.x

Gelman, A., Carlin, J.B., Stern, H.S., Rubin, D.B., 2014. Bayesian data analysis. Chapman & Hall/CRC Boca Raton, FL, USA.

Gradstein, F.M., Ogg, J.G., Smith, A.G., 2004. A Geologic Time Scale 2004. Cambridge University Press.

Hercman, H., Gasiorowski, M., Pawlak, J., 2014. Testing the MOD-AGE chronologies of lake sediment sequences dated by the 210Pb method. *Quaternary Geochronology* 22, 155–162. doi:10.1016/j.quageo.2014.01.001

Hercman, H., Pawlak, J., 2012. MOD-AGE: An age-depth model construction algorithm. *Quaternary Geochronology* 12, 1–10. doi:10.1016/j.quageo.2012.05.003

Huntriss, A., 2008. A Bayesian analysis of luminescence dating (Thesis, NonPeerReviewed).

Kreutzer, S., Fuchs, M., Meszner, S., Faust, D., 2012. OSL chronostratigraphy of a loess-palaeosol sequence in Saxony/Germany using quartz of different grain sizes. *Quaternary Geochronology* 10, 102–109. doi:10.1016/j.quageo.2012.01.004

Lanos, P., Goff, M.L., Kovacheva, M., Schnepf, E., 2005. Hierarchical modelling of archaeomagnetic data and curve estimation by moving average technique. *Geophys. J. Int.* 160, 440–476. doi:10.1111/j.1365-246X.2005.02490.x

Lomax, J., Fuchs, M., Preusser, F., Fiebig, M., 2014. Luminescence based loess chronostratigraphy of the Upper Palaeolithic site Krems-Wachtberg, Austria. *Quaternary International* 351, 88–97. doi:10.1016/j.quaint.2012.10.037

Lu, Y.C., Wang, X.L., Wintle, A.G., 2007. A new OSL chronology for dust accumulation in the last 130,000 yr for the Chinese Loess Plateau. *Quaternary Research* 67, 152–160. doi:10.1016/j.yqres.2006.08.003

Meszner, S., Kreutzer, S., Fuchs, M., Faust, D., 2013. Late Pleistocene landscape dynamics in Saxony, Germany: Paleoenvironmental recon-

- struction using loess-paleosol sequences. *Quaternary International*, Closing the gap - North Carpathian loess traverse in the Eurasian loess belt 6th Loess Seminar, Wrocław, Poland Dedicated to Prof. Henryk Maruszczak 296, 94–107. doi:10.1016/j.quaint.2012.12.040
- Meyers, S.R., Siewert, S.E., Singer, B.S., Sageman, B.B., Condon, D.J., Obradovich, J.D., Jicha, B.R., Sawyer, D.A., 2012. Intercalibration of radioisotopic and astrochronologic time scales for the Cenomanian-Turonian boundary interval, Western Interior Basin, USA. *Geology* 40, 7–10. doi:10.1130/G32261.1
- Millard, A.R., 2006a. Bayesian analysis of ESR dates, with application to Border Cave. *Quaternary Geochronology* 1, 159–166. doi:10.1016/j.quageo.2006.03.002
- Millard, A.R., 2006b. Bayesian Analysis of Pleistocene Chronometric Methods. *Archaeometry* 48, 359–375. doi:10.1111/j.1475-4754.2006.00261.x
- Millard, A.R., 2004. Taking Bayes Beyond Radiocarbon: Bayesian Approaches to Some Other Chronometric Methods, in: Buck, C.E., Millard, A.R. (Eds.), *Tools for Constructing Chronologies*, Lecture Notes in Statistics. Springer London, pp. 231–248.
- Mundil, R., Ludwig K.R., Metcalfe I., Renne P.R., 2004. Age and Timing of the Permian Mass Extinctions: U/Pb Dating of Closed-System Zircons. *Science* 305, 1760–1763. doi:10.1126/science.1101012
- Murray, A.S., Wintle, A.G., 2000. Luminescence dating of quartz using an improved single-aliquot regenerative-dose protocol. *Radiation Measurements* 32, 57–73. doi:10.1016/S1350-4487(99)00253-X
- Preusser, F., Degering, D., Fuchs, M., Hilgers, A., Kadereit, A., Klasen, N., Krubetschek, M., Richter, D., Spencer, J.Q.G., 2008. Luminescence dating: basics, methods and applications. *Eiszeitalter & Gegenwart/Quaternary Science Journal* 57, 95–149. doi:10.3285/eg.57.1-2.5
- R Development Core Team, 2017. R: A Language and Environment for Statistical Computing. <http://r-project.org>
- Rhodes, E.J., Bronk Ramsey, C., Outram, Z., Batt, C., Willis, L., Dockrill, S., Bond, J., 2003. Bayesian methods applied to the interpretation of multiple OSL dates: high precision sediment ages from Old Scatness Broch excavations, Shetland Isles. *Quaternary Science Reviews*, LED 2002 22, 1231–1244. doi:10.1016/S0277-3791(03)00046-5
- Roberts, H.M., 2008. The development and application of luminescence dating to loess deposits: a perspective on the past, present and future. *Boreas* 37, 483–507. doi:10.1111/j.1502-3885.2008.00057.x
- Rousseau, D.-D., Sima, A., Antoine, P., Hatté, C., Lang, A., Zöller, L., 2007. Link between European and North Atlantic abrupt climate changes over the last glaciation. *Geophys. Res. Lett.* 34, L22713. doi:10.1029/2007GL031716
- Sageman, B.B., Singer, B.S., Meyers, S.R., Siewert, S.E., Walaszczyk, I., Condon, D.J., Jicha, B.R., Obradovich, J.D., Sawyer, D.A., 2014. Integrating $^{40}\text{Ar}/^{39}\text{Ar}$, U-Pb, and astronomical clocks in the Cretaceous Niobrara Formation, Western Interior Basin, USA. *Geological Society of America Bulletin* B30929.1. doi:10.1130/B30929.1
- Schnepf, E., Lanos, P., 2005. Archaeomagnetic secular variation in Germany during the past 2500 years. *Geophys. J. Int.* 163, 479–490. doi:10.1111/j.1365-246X.2005.02734.x
- Scholz, D., Hoffmann, D.L., 2011. StalAge – An algorithm designed for construction of speleothem age models. *Quaternary Geochronology* 6, 369–382. doi:10.1016/j.quageo.2011.02.002
- Steier, P., Rom, W., 2000. The use of Bayesian statistics for ^{14}C dates of chronologically ordered samples: A critical analysis. *Radiocarbon* 42, 183–198.
- Telford, R.J., Heegaard, E., Birks, H.J.B., 2004. All age–depth models are wrong: but how badly? *Quaternary Science Reviews* 23, 1–5. doi:10.1016/j.quascirev.2003.11.003
- Timar-Gabor, A., Vandenberghe, D.A.G., Vasiliniuc, S., Panaitiu, C.E., Panaitiu, C.G., Dimofte, D., Cosma, C., 2011. Optical dating of Romanian loess: A comparison between silt-sized and sand-sized quartz. *Quaternary International*, The Second Loessfest (2009) 240, 62–70. doi:10.1016/j.quaint.2010.10.007
- Trandafir, O., Timar-Gabor, A., Schmidt, C.,

Veres, D., Anghelinu, M., Hambach, U., Simon, S., 2015. OSL dating of fine and coarse quartz from a Palaeolithic sequence on the Bistrița Valley (Northeastern Romania). *Quaternary Geochronology*, LED14 Proceedings 30, Part B, 487–492. doi:10.1016/j.quageo.2014.12.005

Újvári, G., Kovács, J., Varga, G., Raucsik, B., Marković, S.B., 2010. Dust flux estimates for the Last Glacial Period in East Central Europe based on terrestrial records of loess deposits: a review. *Quaternary Science Reviews* 29, 3157–3166. doi:10.1016/j.quascirev.2010.07.005

Vibet, M.A., Philippe, A., Lanos, P., Dufresne, P., 2016. ChronoModel V1. 5 User's manual. URL <http://www.chronomodel.fr>.

Wintle, A.G., 1973. Anomalous fading of thermo-luminescence in mineral samples. *Nature* 245, 143–144.